The New Peruvian Meteorite Carancas: Mössbauer Spectroscopy and X-Ray Diffraction Studies

P. Munayco · J. Munayco · M. E. Varela · R. B. Scorzelli

Abstract The Carancas meteorite fell on 15 September 2007 approximately 10 km south of Desaguadero, near Lake Titicaca, Peru, producing bright lights, clouds of dust in the sky and intense detonations. The Carancas meteorite is classified as a H4–5 ordinary chondrite with shock stage S3 and a degree of weathering W0. The Carancas meteorite is characterized by well defined chondrules composed either of olivine or pyroxene. The Mössbauer spectra show an overlapping of paramagnetic and magnetic phases. The spectra show two quadrupole doublets associated to olivine and pyroxene; and two magnetic sextets, associated with the primary phases kamacite/taenite and Troilite (Fe^{2+}). Metal particles were extracted from the bulk powdered samples exhibit only kamacite and small amounts of the intergrowth tetrataenite/antitaenite. X-Ray diffractogram shows the primary phases olivine, pyroxene, troilite, kamacite, diopside and albite. Iron oxides has not been detected by Mössbauer spectroscopy or XRD as can be expected for a meteorite immediately recovered after its fall.

Keywords Peruvian meteorite · Chondrite · Carancas · Mössbauer spectroscopy

1 Introduction

Chondrites are the most numerous meteorite group, accounting for 87 % of all meteorites observed to fall. As a rock type, chondrites are highly heterogeneous and more than 10 distinct groups can be distinguished. The largest group, collectively known as the ordinary chondrites (OC), account for 80 % of all known meteorites. The OC consist exclusively of anhydrous minerals (principally olivine, pyroxenes, troilite, and Fe–Ni metal) and formed under intermediate redox conditions. Consequently, the iron present is distributed between

P. Munayco (✉) · J. Munayco · R. B. Scorzelli
Centro Brasileiro de Pesquisas Físicas (CBPF/MCT), Rua Xavier Sigaud 150,
Rio de Janeiro 22290-180, Brazil
e-mail: mpablo@cbpf.br

M. E. Varela
Instituto de Ciencias Astronómicas de la Tierra y del Espacio (ICATE/CONICET),
Av. España 1512 Sur, CPJ5402DSP San Juan, Argentina

the silicates (dissolved as iron oxide), sulfides, and metal. According to the bulk content of Fe, the amount of metal present, and the amount of FeO present in the silicates (in order of increasing FeO contents) we distinguish three sub groups: H group (high iron), L group (low iron), and LL group (low total iron, low metal). The classification scheme for chondrites (Van Schmus and Wood 1967) links the degree of chemical homogenization of the major silicates to the degree of recrystallization. Accordingly, the petrologic types 4–6, which comprise the equilibrated ordinary chondrites (EOC), will exhibit moderate (type 4) to strong (type 6) degree of recrystallization and corresponding alteration of their textural features. Here, we have adopted an empirical approach which utilizes the fact that all the iron in an EOC is present as Fe^{2+} (in silicates and sulphides) or Fe^0 (in Fe–Ni metal).

In this paper, we use ^{57}Fe Mössbauer spectroscopy and X-ray diffraction to study the Carancas meteorite fall. Considering that Mössbauer is a powerful tool for detecting Fe-bearing phases, and taking into account that OCs are made up of minerals all of which contain Fe (e.g., olivine, pyroxene, troilite and Fe–Ni), more than 90 % of their mineralogy can be detected by this technique. In addition, Mössbauer spectroscopy is extremely sensitive to changes in Fe valence state, and allows the relative proportion of Fe-bearing phases to be quantified. X-Ray diffraction provides a means of characterizing and quantifying mineral phases (Fe-bearing and Fe-free) in meteorites.

2 Carancas Meteorite

The Carancas meteorite fell on 15 September 2007 approximately 10 km south of Desaguadero, near Lake Titicaca, Peru, producing bright lights, clouds of dust in the sky and intense detonations. The meteorite excavated a crater about 15 m in diameter, at 3,826 m altitude (coordinates 16°39′52″S, 69°02′38″W), formed as a result of a hypervelocity impact (Brown et al. 2008, Tancredi et al. 2009). The estimated timing of the fall was recorded at approximately 11:40 AM (local time) (16:40 UT). The fireball trajectory was roughly estimated from east to west, with an inclination between 45° and 60° measured from the horizontal (Tancredi et al. 2009).

The Carancas meteorite is classified as a H4–5 ordinary chondrite with shock stage S3, a degree of weathering W0 and the total mass is currently unknown (Connolly 2007).

After Carancas fall, the media reported that hundreds of people got sick while visiting the crater. Tancredi et al. (2009) concluded that there were no firm evidence to suggest that more than a few persons were affected by the gases liberated at impact. These gases, which were trapped below the surface, were released through the bubbling of the groundwater that covered the crater floor. But the water was not boiling and the crater was not steaming (Tancredi et al. 2009). Most of the alleged health problems were a consequence of mass hysteria and people seeking free medical support for pre-existing conditions.

3 Petrography and Mineral Chemistry

Several samples of the grayish material found close to the crater were collected a few minutes after the fall. The petrographic and electron microprobe analysis were performed on two thin sections of the meteorite fragments. The samples were investigated with an optical microscope and analytical scanning electron microscope JEOL 6400. Major element composition was determined with an ARLSEMQ electron microprobe (Naturhistorisches Museum, Vienna, Austria) operated at 15 kV accelerating voltage and 15 nA sample current. The online ZAF program was used for corrections.
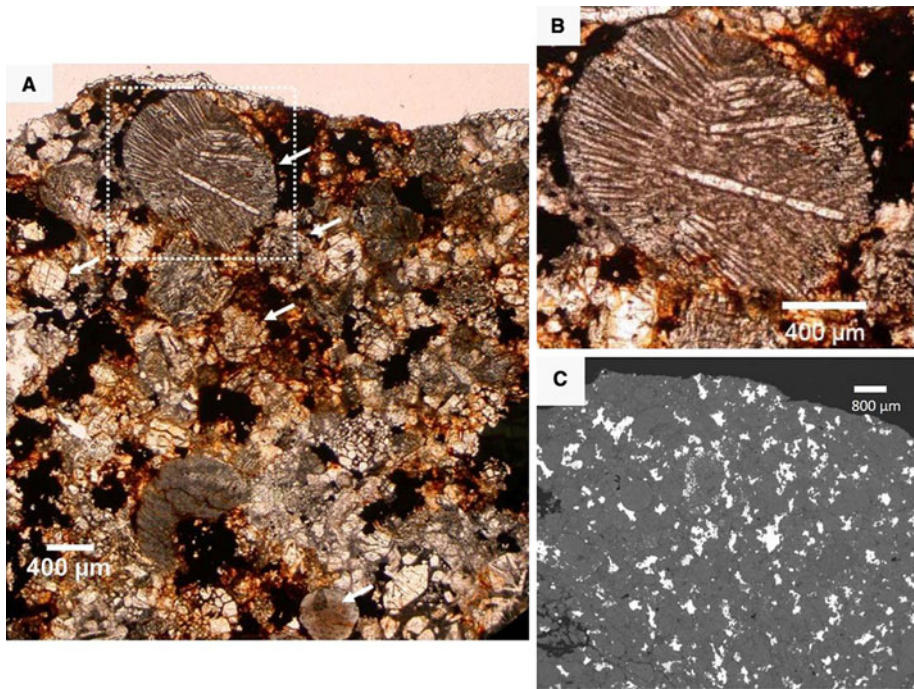
Fig. 1 **a** Transmitted light optical image showing the texture of the Carancas H4–5 ordinary chondrite in which several spherical chondrules are clearly observed (indicated by white arrows). Scale (white bar):400 μm. **b** Detail of the inset in A showing a radiating pyroxene composite chondrule (plane-polarized light). Scale: 400 μm. **C** Backscatter electron (BSE) image showing the abundance of metal and sulfides in Carancas, Scale: 800 μm

The Carancas meteorite is characterized by well defined chondrules (round objects indicated by white arrows in Fig. 1a) composed mainly of olivine (central and left objects) or pyroxene (lower and central objects). Some of these chondrules, mainly composed of radiating pyroxenes, can form compound chondrules, as that observed in Fig. 1b. The clear grains observed in the lower left corner of Fig. 1b are olivine-rich objects. All black irregular grains in both images (Fig. 1a, b) correspond to metal and sulfides. The same phases are clearly observed as white irregular grains in the backscatter electron image (Fig. 1c), emphasizing the abundance of the metal phase in Carancas. Taking into account the meteorite texture, the minor amount of clinopyroxene as well as the relatively uniform composition of ferromagnesian minerals: olivine and pyroxene (ferrosilite in orthopyroxene: mol % 16.7; fayalite in olivine: mol % 18) the Carancas meteorite was classified as an H4–5 ordinary chondrite, in concordance with Connolly (2007). Representative and averaged electron microprobe analyses (EMPA) of the phases are given in Table 1.
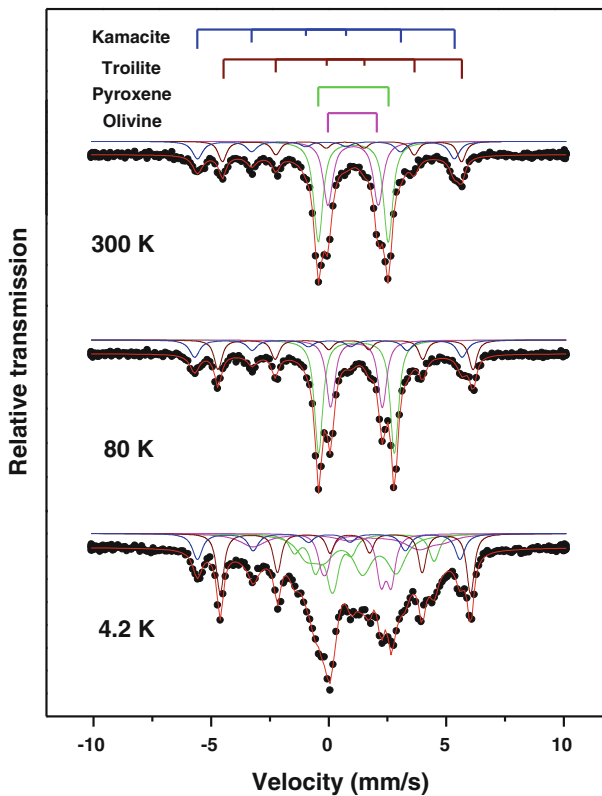
4 Mössbauer Spectroscopy

^{57}Fe Mössbauer spectroscopy in transmission geometry was performed at room temperature (RT) and low temperature (80 and 4.2 K) in a 512 channels Halder spectrometer. The drive velocity was calibrated using a ^{57}Co in Rh matrix source and an iron foil both at RT.

Table 1 Representative major element composition of olivine (Ol) and pyroxene (Px) in Carancas (EMPA in wt %)

	Ol	D. std	Px	D. std
N	10		10	
SiO_2	38.5	1.09	55.2	1.10
Al_2O_3	0.01	0.50	0.49	0.51
TiO_2	0.01	0.08	0.14	0.08
Cr_2O_3	0.01	0.60	0.57	0.60
MnO	0.47	0.03	0.50	0.03
FeO	17.4	0.31	10.9	0.31
CaO	0.00	0.20	0.64	0.20
MgO	43.7	1.08	31.0	1.08
Total	100.1		99.4	

All measurements were performed at high velocity (10 mm/s), average recording time of 24 h per sample. Mössbauer absorbers were prepared with 90 mg/cm^2 of the bulk meteorite sample. NORMOS code (Brand 1995) was used for the spectrum analysis based on least-square fitting routine, assuming each spectrum to be a sum of Lorentzian lines

Fig. 2 Mössbauer spectra obtained at different temperatures of the Carancas meteorite indicating the presence of primary phases: olivine, pyroxene, troilite and kamacite/taenite

grouped into quadrupole doublets and magnetic sextets. The isomer shifts was reported in relation to α-Fe.

The Mössbauer spectra at 300 and 80 K show an overlapping of paramagnetic and magnetic phases as observed in Fig. 2. The spectra were fitted with two quadrupole doublets attributed to Fe^{2+}: one associated with olivine and the other to pyroxene; and two magnetic sextets, associated with the primary phases kamacite/taenite (Fe^{0+}) and Troilite (Fe^{2+}) (Stevens et al. 1998).

Mössbauer spectra at 4.2 K exhibit a too complex spectra due to relaxation effects (Munayco et al. 2011) exhibiting the same components as at RT: olivine, pyroxene, troilite and kamacite/taenite. In order to take into account the relaxation effects due to olivine and pyroxene, it was necessary to use the spherical relaxation model of the fitting program Normos considering two different components for olivine and pyroxene, in accordance with two different crystallographic sites occupied by iron atoms. The hyperfine parameters obtained from the fitting of the spectra (Fig. 2) are shown in Table 2a.

In order to better define the Fe–Ni phases, the metal particles were extracted from the bulk powdered samples by grinding the meteorite fragments under acetone followed by magnetic separation with a hand magnet. The magnetic fraction is submitted to further grinding and magnetic separation under acetone in order to purify the metal grains from

Table 2 Hyperfine parameters and relative areas at different temperatures of Carancas meteorite (a) bulk, (b) metal particles, (c) metal particles after chemical treatment

T (K)	Mineral phase	IS (mm/s)	QS (mm/s)	B_{hf} (T)	ω (Mhz)	Area (%)
(a) Bulk						
300	Olivine	1.16	2.97	–	–	41.0
	Pyroxene	1.15	2.14	–	–	28.0
	Troilite	0.75	−0.07	31.5	–	15.0
	Kamacite/taenite	0.01	0.00	33.8	–	16.0
80	Olivine	1.30	3.22	–	–	40.0
	Pyroxene	1.30	2.20	–	–	25.0
	Troilite	0.90	0.07	32.6	–	20.0
	Kamacite/taenite	0.13	−0.03	34.3	–	15.0
4.2	Olivine 1	0.91	2.73	4.5	3.0	25.0
	Olivine 2	1.18	2.62	13.1	0.4	18.0
	Pyroxene 1	1.24	2.63	1.3	0.4	14.0
	Pyroxene 2	1.24	2.53	22.0	6.0	12.0
	Troilite 1	0.92	−0.09	33.0	–	19.0
	Kamacite/taenite	0.13	−0.01	34.7	–	12.0
(b) Metal particles						
300	Kamacite	0.02	0.00	33.2		90.0
	Antitaenite	0.07	–	–		6.0
	Tetrataenite	0.05	0.20	29.4		4.0
(c) Metal particles after chemical treatment						
300	Kamacite	0.08	0.06	33.5		26.0
	Antitaenite	−0.03	–	–		25.0
	Ordered Tetrataenite	0.08	0.22	29.2		29.0
	Disordered Tetrataenite	0.08	0.00	31.2		20.0
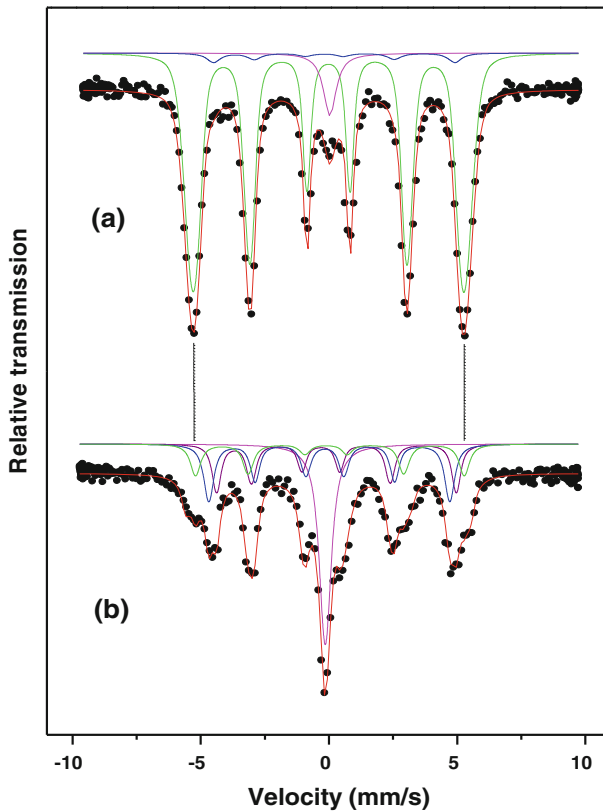
Fig. 3 Mössbauer spectra of Carancas meteorite: **a** metal particles showing kamacite, antitaenite and tetrataenite, **b** metal particles after chemical treatment showing kamacite, antitaenite and ordered and disordered tetrataenite

silicates and troilite particles. The Mössbauer spectra of these particles (Fig. 3a) free of silicates and troilite, exhibit only kamacite and small amounts of the intergrowth tetrataenite/antitaenite (Rancourt and Scorzelli 1995). Hyperfine parameters are presented in Table 2b.

The metal particles are then submitted to chemical treatment with HCl (1 M) for 24 h. The Mössbauer spectra of these particles show an important decrease in the relative proportion of kamacite and two magnetic components attributed to ordered and disordered tetrataenite and a single line corresponding to antitaenite (Fig. 3b; Table 3c).
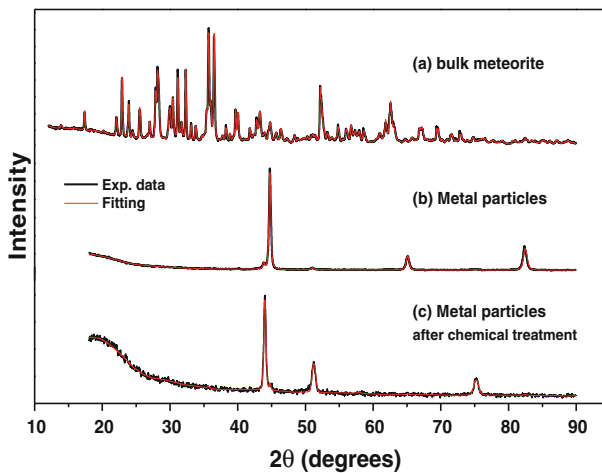
5 X-Ray Diffraction

X-Ray diffraction (XRD) measurements were performed in a Panalytical X″ Pert pro diffractometer with a solid state detector and acquisition time of 300 s using Cu-Kα radiation and 2θ range from 20° to 90°.

Rietveld refinement was done with the MAUD software (Lutterotti 2010) with pseudo-Voigt function to describe the peaks and a Caglioti function to describe the full width half

Table 3 Lattice parameters and the weight percentage of the different phases of Carancas meteorite: (a) bulk, (b) metal particles, (c) metal particles after chemical treatment

Mineral phase	Composition	a (Å)	b (Å)	c (Å)	α (°)	β (°)	ϒ (°)	wt (%)	at. % Fe
(a) Bulk									
Olivine	$(Mg_{0.816}Fe_{0.184})_2Si_4O_6$	4.767	10.254	6.004	90	90	90	44.0	43.0
Orthopyroxene	$(Mg_{0.839}Fe_{0.161})_2Si_2O_6$	18.267	8.852	5.198	90	90	90	38.0	24.0
Troilite	FeS	5.955	5.955	11.730	90	90	120	3.0	16.0
Kamacite	$Fe_{0.9}Ni_{0.1}$	2.865	2.865	2.865	90	90	90	2.0	17.0
Diopside	$MgCaSi_2O_6$	9.725	8.918	5.261	90	106.05	90	7.0	–
Albite	$NaAlSi_3O_8$	8.159	12.842	7.131	93.14	116.44	89.89	6.0	–
(b) Metal particles									
Kamacite	$Fe_{0.9}Ni_{0.1}$	2.865	2.865	2.865	90	90	90	87	92.5
Tetrataenite	$Fe_{0.5}Ni_{0.5}$	3.567	3.563	3.591	90	90.27	90	13	7.5
(c) Metal particles after chemical treatment									
Kamacite	$Fe_{0.9}Ni_{0.1}$	2.866	2.866	2.866	90	90	90	3.5	6.0
Tetrataenite	$Fe_{0.5}Ni_{0.5}$	3.565	3.569	3.580	90	90.25	90	96.5	94.0

Fig. 4 X-Ray diffractogram of Carancas meteorite **a** bulk meteorite, **b** metal particles. The *red line* indicate the Rietveld method fitting

maximum as a function of the angle. The compositions of all phases were kept constant during the least square fitting, however the iron content in the olivine and pyroxene were properly adjusted to the values found by microprobe.

X-Ray diffractogram for the Carancas meteorite can be seen in Fig. 4. The XRD allowed the discrimination and quantification of the iron and the non-iron phases. Up to six different phases were considered during the Rietveld modeling (Toby 2006). The fitting results can be seen in Fig. 4a.

The comparison of phase quantification obtained by XRD and Mössbauer was done with the necessary conversion of the XRD results from weight percentage to molar percentage of iron, using the iron percentage inside each crystalline phase system, the number of molecules inside the unit cell and total cell mass of each phase. These comparisons for silicates (olivine and orthopyroxene) and opaque minerals (kamacite and troilite) expressed in at. % Fe show good agreement between Mössbauer and XRD methods (Tables 2, 3).

X-Ray diffractogram of the magnetic fraction show only the presence of kamacite and tetrataenite. After chemical treatment, mainly tetrataenite is observed and small amounts of kamacite in agreement with Mossbauer spectroscopy. The results are shown in the Table 3b, c.

6 Conclusions

The petrographic and chemical studies of the thin sections allow the classification of the Carancas meteorite as an H4–5 ordinary chondrite, in concordance with previous results.

The principal phases in the Carancas meteorite identified by Mössbauer spectroscopy and X-ray diffraction are olivine (Fe^{2+}), orthopyroxene (Fe^{2+}), troilite (Fe^{2+}), Fe–Ni phases (Fe^0), albite and diopside. The Fe–Ni phases are kamacite and the intergrowth tetrataenite/antitaenite.

Iron oxides have not been observed by Mössbauer spectroscopy or XRD as can be expected for a meteorite immediately recovered after its fall, as is the case of the Carancas meteorite. Weathering processes require a certain time to transform the primary phases in iron oxides.

To study the Fe–Ni phases, especially the intergrowth tetrataenite/antitaenite it is only possible by extraction of the metal particles from de bulk sample followed by chemical treatment in order to reduce or eliminate the kamacite.

In this study, we have not observed the presence of polymorph phases of olivine associated with shock effects. This is coherent with the degree of shock S3 of the Carancas meteorite which is insufficient to produce effects in the target minerals.

References

W.R. Van Schmus, J.A. Wood, A chemical-petrographic classification for the chondritic meteorites. Geochim. Cosmochim. Acta **31**, 747–765 (1967)

P. Brown, E.A. Sukara, D.O. ReVelle, W.N. Edwards, S. Arrowsmith, L. Jackson, G. Tancredi, D. Eaton, Analysis of a crater-forming meteorite impact in Peru. J. Geophys. Res. **113**, E09007, 13 (2008). doi: 10.1029/2008JE003105

G. Tancredi, J. Ishitsuka, P.H. Schultz, R.S. Harris, P. Brown, D.O. Revelle, K. Antier, A. Le Pichon, D. Rosales, E. Vidal, M.E. Varela, L. Sánchez, S. Benavente, J. Bojorquez, D. Cabezas, A. Dalmau, A meteorite crater on Earth formed on september 15, 2007: the carancas hypervelocity impact. meteorit. Planet. Sci. **44**(12), 1967–1984 (2009)

H. Connolly, Meteoritical bulletin, No. 93. Meteorit. Planet. Sci. **43**, 571–632 (2007)

R.A. Brand, *Normos Mössbauer Fitting Program, User's Guide* (Wissenschaftlich Elektronik GmbH, Starnberg, 1995)

J.G. Stevens, A.M. Khasanov, J.W. Miller, H. Pollak, Z. Li, *Mössbauer Mineral Handbook* (Mössbauer effect Data Center, The University of North Carolina at Asheville, USA, 1998)

P. Munayco, J. Munayco, R.R. Avillez, M. Valenzuela, J. Gattacceca, P. Rochette, R.B. Scorzelli, Synchrotron X-ray diffraction and mössbauer spectroscopy studies of weathering effects on ordinary chondrites from the atacama desert. Chile. Meteorit. Planet Sci. **46**, A169–A169 (2011)

D.G. Rancourt, R.B. Scorzelli, J. Magn. Magn. Mater. **150**, 30–36 (1995)

L. Lutterotti, Total pattern fitting for the combined size-strain-stress-texture determination in thin film diffraction. Nucl. Instrum. Meth. B **268**, 334–340 (2010)

B.H. Toby, *R* factors in Rietveld analysis: how good is good enough? Powder Diffr. **21**(1), 67–70 (2006)